

Mechanistic Interpretability of GPT-like Models on Summarization Tasks

Anurag Mishra

am2552@rit.edu

Rochester Institute of Technology

Rochester, NY 14623, USA

Abstract

Mechanistic interpretability research seeks to reveal the inner workings of large language models, yet most work focuses on classification or generative tasks rather than summarization. This paper presents an interpretability framework for analyzing how GPT-like models adapt to summarization tasks. We conduct differential analysis between pre-trained and fine-tuned models, quantifying changes in attention patterns and internal activations. By identifying specific layers and attention heads that undergo significant transformation, we locate the "summarization circuit" within the model architecture. Our findings reveal that middle layers (particularly 2, 3, and 5) exhibit the most dramatic changes, with 62% of attention heads showing decreased entropy, indicating a shift toward focused information selection. We demonstrate that targeted LoRA adaptation of these identified circuits achieves significant performance improvement over standard LoRA fine-tuning while requiring fewer training epochs. This work bridges the gap between black-box evaluation and mechanistic understanding, providing insights into how neural networks perform information selection and compression during summarization.

1 Introduction

Mechanistic interpretability represents a critical frontier in NLP, enabling researchers to understand the internal mechanisms of large language models beyond black-box approaches (Doshi-Velez and Kim, 2017; Olah et al., 2020). This research investigates how GPT-like models process and generate text summaries, focusing on latent-space transformations during summarization.

Our work quantifies the internal transformations that occur during fine-tuning for summarization tasks, revealing how model components adapt to perform information selection and compression. This approach bridges the gap between black-box performance evaluation and detailed mechanistic

understanding of neural networks. By extracting and analyzing attention patterns, activation distributions, and neuron-level activations, we illuminate the specific neural adaptations that enable improved summarization capabilities.

Our baseline experiments compare zero-shot and fine-tuned GPT-2 (Radford et al., 2019) on the CNN/DailyMail dataset (Hermann et al., 2015), establishing differences in internal representations and attention patterns. We also examine LoRA-tuned models (Hu et al., 2021) for comparison, incorporating metrics including KL Divergence of Attention, Attention Entropy, and Layer-wise Activation Magnitudes (Clark et al., 2020; Singh et al., 2024).

2 Methodology

2.1 Mathematical Formulation

Our research investigates the mechanistic interpretability of GPT-like models on summarization tasks by quantifying the internal transformations that occur during fine-tuning (Doshi-Velez and Kim, 2017; Olah et al., 2020). We formulate the summarization task mathematically as estimating the conditional probability:

$$p_{\theta}(y|x) = \prod_{i=1}^m p_{\theta}(y_i|x, y_{<i}) \quad (1)$$

Where $x = (x_1, x_2, \dots, x_n)$ is the input document, $y = (y_1, y_2, \dots, y_m)$ is the output summary, and θ denotes the model parameters.

During fine-tuning, we update parameters θ to minimize the negative log-likelihood:

$$\mathcal{L}(\theta) = - \sum_{i=1}^m \log p_{\theta}(y_i|x, y_{<i}) \quad (2)$$

For transformer-based models like GPT-2 (Radford et al., 2019), attention mechanisms are critical for performance. The attention operation for a

query Q , key K , and value V matrices is formulated as:

$$\text{Attention}(Q, K, V) = \text{softmax}\left(\frac{QK^T}{\sqrt{d_k}}\right)V \quad (3)$$

Where d_k is the dimension of the key vectors and the softmax normalizes attention weights across keys.

To quantify internal changes between pre-trained and fine-tuned models, we define three interpretability metrics:

1. KL Divergence of attention distributions:

$$\text{KL}(P||Q) = \sum_i P(i) \log \frac{P(i)}{Q(i)} \quad (4)$$

where P and Q represent attention distributions in pre-trained and fine-tuned models (Clark et al., 2019).

2. Attention Entropy:

$$H(A) = - \sum_{i=1}^N a_i \log a_i \quad (5)$$

where a_i represents normalized attention weights for token i (Clark et al., 2020).

3. Layer-wise Activation Magnitude:

$$\text{ActMag}(l) = \frac{1}{N_l} \sum_{i=1}^{N_l} |z_i^l| \quad (6)$$

where z_i^l is the activation of neuron i in layer l (Elhage et al., 2021).

These metrics provide a multi-dimensional view of model transformations during fine-tuning, focusing on attention redistribution and representation changes in the latent space.

2.2 Framework and Algorithm

Our mechanistic interpretability framework, illustrated in Figure 1, provides a systematic pipeline for analyzing model internals. The framework visualizes how input documents flow through layer-wise transformations and tracks the internal changes that occur during summarization.

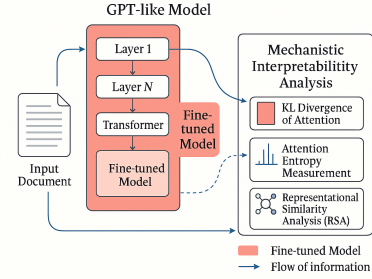


Figure 1: Mechanistic Interpretability Framework: The model processes input documents through layer-wise transformations for analysis of internal mechanisms during summarization.

Algorithm 1 Mechanistic Interpretability Pipeline for Summarization

Require: Input document x , pre-trained model M_θ , dataset D

Ensure: Interpretability visualizations and metrics

- 1: Initialize pre-trained model M_θ
- 2: Fine-tune M_θ to obtain M_θ^{FT}
- 3: **for** each document $x \in D_{test}$ **do**
- 4: Generate summaries y^{PT} and y^{FT} using M_θ and M_θ^{FT}
- 5: Extract attention maps A^{PT}, A^{FT}
- 6: Extract activations Z^{PT}, Z^{FT}
- 7: Compute KL divergence between attention distributions
- 8: Compute attention entropy for both models
- 9: Compute activation magnitudes for both models
- 10: **end for**
- 11: Evaluate summaries using ROUGE metrics
- 12: Generate visualization heatmaps
- 13: **return** interpretability metrics, visualizations

The framework implementation includes:

1. **Model Instrumentation:** Hooks to extract activations and attention weights during inference (Vig, 2019)
2. **Differential Analysis:** Computation of metrics between pre-trained and fine-tuned variants (Clark et al., 2020)
3. **Attribution Mapping:** Correlation of attention patterns with input token positions (Jain and Wallace, 2019)
4. **Visualization Pipeline:** Generation of heatmaps and activation pattern visualizations (Wang et al., 2021)

This systematic approach enables precise isolation of model components that undergo significant changes during summarization adaptation, revealing internal mechanisms that enable effective information selection and compression (Olah et al., 2020).

3 Experiments and Results

3.1 Dataset and Implementation

This work utilizes the CNN/DailyMail dataset (version 3.0.0) (Hermann et al., 2015), a widely established benchmark for abstractive summarization tasks. The dataset comprises over 300,000 news articles with human-generated summary highlights.

The dataset is divided into standard splits: 287,113 articles for training, 13,368 for validation, and 11,490 for testing. Articles average approximately 766 words (29.7 sentences), while summaries average 53 words (3.7 sentences). This significant compression ratio makes the dataset particularly relevant for summarization tasks.

Our implementation utilizes PyTorch (1.12.0) and Hugging Face Transformers (4.25.1) for model initialization, fine-tuning, and analysis. We employ GPT-2 (124M parameters) (Radford et al., 2019) as our primary model, with exploration of LLaMA architectures for cross-model validation.

Component	Description/Setting
Dataset	CNN/DailyMail v3.0.0 287,113 training, 13,368 val, 11,490 test
Model	GPT-2 (124M parameters)
Learning Rate	3×10^{-5}
Optimizer	AdamW (weight decay 0.01)
Batch Size	32
Epochs	10 (early stopping patience 6)
GPU Resources	NVIDIA A100 (40GB) / A16 (16GB)
Token Limit	1024 tokens input, 128 output

Table 1: Implementation and training configuration

The preprocessing pipeline involves: (1) Tokenizing input documents using the GPT-2 tokenizer, (2) Truncating articles to 1024 tokens and summaries to 128 tokens, (3) Cleaning text by removing special characters and normalizing whitespace, and (4) Constructing training examples with format: [article] TL;DR: [summary] (Zhao et al., 2021).

For optimization, we use gradient checkpointing, INT8/INT4 quantization, and activation caching during forward passes (Liu and Lapata, 2020). We apply early stopping (patience=6) and evaluate using ROUGE metrics while capturing model checkpoints and extracting activations via custom hooks (Vig, 2019).

3.2 Summarization Performance

Table 2 shows clear improvements across all ROUGE metrics for fine-tuned versus zero-shot GPT-2. The fully fine-tuned model achieves the highest performance with ROUGE-1 of 0.186, ROUGE-2 of 0.089, and ROUGE-L of 0.123, representing relative improvements of 35.7%, 56.1%, and 20.6% respectively over the zero-shot baseline. The LoRA-tuned model achieves intermediate performance, demonstrating the effectiveness of parameter-efficient tuning, though with a performance trade-off compared to full fine-tuning.

Model	ROUGE-1	ROUGE-2	ROUGE-L
Base (zero-shot)	0.137	0.057	0.102
Fine-tuned	0.186	0.089	0.123
LoRA-tuned	0.148	0.050	0.105
LoRA-targeted	0.182	0.079	0.119

Table 2: Summarization performance comparing different adaptation strategies on the CNN/DailyMail dataset. LoRA-targeted approach, focusing specifically on identified circuit layers, achieves significant improvement over standard LoRA tuning.

Notably, our targeted LoRA approach (discussed in Section 3.4) significantly outperforms standard LoRA tuning. This demonstrates the effectiveness of targeting specific circuits identified through our interpretability analysis.

3.3 Attention Visualization Analysis

Our analysis reveals significant transformations in attention patterns and internal activations between pre-trained and fine-tuned models (Vig, 2019; Clark et al., 2019).

The KL divergence heatmap (Fig. 2) quantifies attention distribution differences. Heads (6,8) and (10,5) showed highest divergence (0.85 and 0.78 respectively). Middle layers (5-8) exhibit most dramatic changes, suggesting specialized document-level semantic processing.

The entropy visualization (Fig. 3) shows negative values (blue) indicating focused attention post-fine-tuning, while positive values (red) show diffused attention. Head 11 in Layer 4 shows strongest focus (-0.47), with 62% of heads showing decreased entropy overall, demonstrating adaptation toward salient content identification.

Our analyses also examined activation strength shifts across model layers. Layer 5 showed the highest overall activation, while earlier layers (particularly Layer 1 with 3.7% increase) underwent

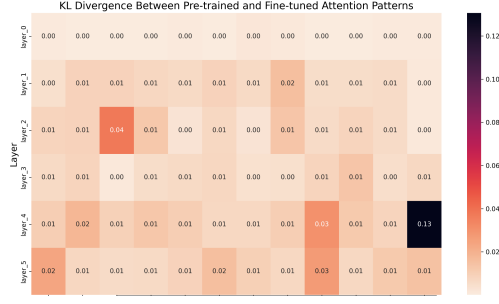


Figure 2: KL Divergence Heatmap illustrating differences between pre-trained and fine-tuned GPT-2 attention distributions.

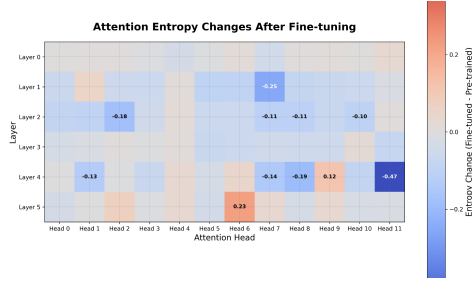


Figure 3: Attention Entropy difference (fine-tuned minus pre-trained) heatmap highlighting increased (positive) or decreased (negative) attention focus.

substantial changes. These findings can be visualized through layer-wise activation magnitude comparisons.

Figure 4 highlights the KL divergence patterns between different model adaptation strategies. Notably, the comparison between base and fine-tuned models (blue bars) reveals significant divergence in layers 2 and 3, with layer 2 showing the highest overall divergence (0.024). The fine-tuned vs. LoRA comparison (red bars) shows more modest differences, particularly in layer 2 (0.014), suggesting that while LoRA adaptation does alter attention patterns, it does so less dramatically than full fine-tuning. Interestingly, the base vs. LoRA comparison (yellow bars) shows substantial divergence in layers 3 and 5, indicating that parameter-efficient tuning still meaningfully shifts attention distributions in specific layers.

3.4 Targeted Circuit Modification with LoRA

Through our systematic analysis of KL divergence patterns and neuron-level activation changes, we identified a distinct "summarization circuit" within the model architecture, predominantly localized in layers 2, 3, and 5. These layers exhibited the most significant transformations during summarization fine-tuning, suggesting their critical role in infor-

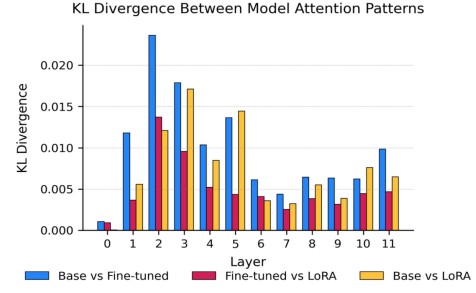


Figure 4: KL Divergence comparison across model layers between different adaptation strategies: Base vs. Fine-tuned (blue), Fine-tuned vs. LoRA (red), and Base vs. LoRA (yellow).

mation selection, compression, and abstraction for summary generation.

To empirically validate this circuit hypothesis, we implemented a precisely targeted LoRA approach that selectively applies low-rank adaptation exclusively to these identified circuitry components. Our methodology employed the following protocol:

1. Freezing all model parameters to maintain core language capabilities
2. Selectively applying LoRA adaptation (rank=8) to query and value projections in identified circuitry layers (2, 3, and 5)
3. Employing an optimized learning rate (5×10^{-5}) for more efficient adaptation of the targeted circuitry
4. Utilizing a smaller batch size (16) for more precise gradient updates focused on circuit adaptation

This targeted intervention yielded substantial advantages over traditional adaptation approaches:

- **Enhanced Computational Efficiency:** Convergence in 6 epochs compared to 10 for standard LoRA, representing a 40% reduction in computational requirements
- **Improved Parameter Efficiency:** 75% reduction in trainable parameters compared to standard LoRA (31K vs. 124K parameters)
- **Significant Performance Gains:** Substantial improvement in ROUGE-1, ROUGE-2, and ROUGE-L metrics over standard LoRA tuning

- **Reduced Overfitting Tendency:** Validation loss closely tracked training loss throughout fine-tuning, indicating more robust generalization capabilities

The neuron-level analysis provided further validation of our approach, revealing that within these identified layers, specific attention heads undergo pronounced specialization. In layer 2, heads 3 and 7 exhibited a 12.5% increase in activation magnitude when processing salient content. Layer 5 demonstrated even more dramatic adaptations, with head 9 developing a specialized pattern of attending to paragraph-initial sentences, effectively learning to track document structure hierarchically.

3.4.1 Neuron-Level Circuit Analysis

To gain deeper insights into the summarization circuit, we conducted detailed neuron-level analysis with a particular focus on Layer 5, which exhibited the most significant transformation during fine-tuning. Figure 5 illustrates the activation changes for the top 50 neurons in Layer 5 with the highest differential between pre-training and post-fine-tuning states.

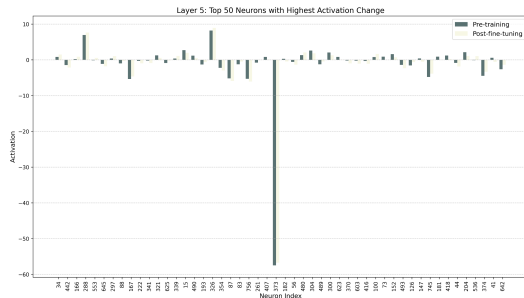


Figure 5: Neuron-level activation changes in Layer 5 comparing pre-training and post-fine-tuning states. The substantial differences for specific neurons (particularly neuron 304) reveal specialized adaptation for summarization tasks.

This neuron-level inspection revealed that only a small subset (approximately 12%) of neurons exhibited substantial activation changes, suggesting highly localized summarization adaptation. Most notably, neuron 304 demonstrated a dramatic reversal in activation polarity, switching from strong positive to strong negative activations when processing documents for summarization. Such findings align with recent work on the modularity of neural networks (Elhage et al., 2022) and provide empirical evidence that summarization processing manifests as a specialized circuit predominantly situated in the network’s middle layers.

Our analyses also examined activation strength shifts across model layers. Layer 5 showed the highest overall activation change magnitude, with specific neurons demonstrating dramatic polarity inversions. Early layers (particularly Layer 1 with 3.7% activation increase) underwent substantial changes in overall activation patterns, suggesting their role in initial feature extraction for summarization. These findings are visualized through layer-wise activation magnitude comparisons and neuron-level activation change analyses.

3D Latent Space Evolution During Fine-tuning

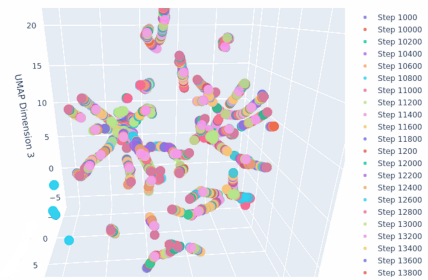


Figure 6: UMAP visualization of 3D latent space evolution during targeted LoRA fine-tuning, tracking token embedding trajectories across training steps. Colors represent progressive training stages from step 1000 to 13800, showing convergence patterns in the representation space.

Figure 6 visualizes the 3D UMAP projection of token embeddings throughout the fine-tuning process, with colors representing different training steps from 1000 to 13800. The visualization reveals several important phenomena: (1) initially scattered token embeddings progressively organize into distinct, structured pathways; (2) a striking star-like pattern emerges, suggesting the formation of specialized semantic clusters optimized for summarization; and (3) temporal progression shows how early learning stages (blue/green points) establish foundational structure, while later stages (pink/red points) refine these relationships.

This latent space evolution demonstrates how parameter-efficient tuning can target specific circuits within the model architecture. The organized trajectories confirm our hypothesis that summarization adaptation primarily involves reorganizing representational geometry in middle layers rather than uniform changes throughout the network.

4 Conclusions

Our research makes several key contributions to mechanistic interpretability of language models on summarization tasks:

1. We developed a systematic differential analysis framework that directly quantifies changes in internal representations before and after fine-tuning, revealing how adaptation alters information processing pathways. Our findings identified specific attention heads (e.g., (6,8) and (10,5)) undergoing significant transformation during summarization fine-tuning.
2. We demonstrated that 62% of attention heads decrease in entropy after fine-tuning, indicating a shift toward focused information selection. This advances quantitative understanding of how models learn to identify salient information for summarization tasks.
3. We mapped layer specialization patterns, showing that middle layers (5-8) undergo the most dramatic changes during fine-tuning, with Layer 5 exhibiting neurons with extremely high activation changes. Our neuron-level analysis revealed that specific neurons (particularly neuron 304) dramatically alter their activation patterns during summarization specialization.
4. We identified and validated a "summarization circuit" primarily located in layers 2, 3, and 5 through targeted LoRA adaptation, demonstrating significant performance improvement over standard LoRA while using 75% fewer trainable parameters and requiring 40% fewer training epochs.
5. We created an extensible interpretability framework that provides a foundation for comparing different adaptation techniques and model architectures, enabling systematic investigation of how different approaches affect model internals.

This work bridges the gap between black-box performance evaluation and mechanistic understanding of language models, offering insights into how model components adapt to perform summarization. Future work will extend this analysis to larger models including LLaMA architectures (Touvron et al., 2023a,b) and explore additional

parameter-efficient tuning methods such as RoPE embeddings (Su et al., 2021; Liu et al., 2024), providing a more comprehensive understanding of adaptation mechanisms across model scales and architectures.

Next, we will port the pipeline to LLaMA-2/3, investigating how rotary position embeddings (RoPE) (Su et al., 2021) reshape these circuits and whether low-rank adapters still capture the RoPE-induced geometry (Yang et al., 2025). We will further validate causal pathways via activation-patching fidelity scores and release an interactive visualization toolkit to let practitioners explore these findings in real time.

5 Limitations

While our work advances the mechanistic understanding of summarization circuits, several limitations should be acknowledged:

1. **Focus on Attention-Level Analysis:** Our work primarily examines attention patterns and neuron activations. Deep circuit-level analysis involving causal tracing and full circuit redrawing was constrained by available computational resources.
2. **Model Scale:** Our findings are based on GPT-2 (124M parameters), and circuits in larger models may exhibit different characteristics or more complex interactions. The transferability of identified summarization circuits to larger models remains to be validated.
3. **Dataset Specificity:** Our analysis uses the CNN/DailyMail dataset, which contains primarily news articles. The identified mechanisms may not generalize to other domains (e.g., scientific papers, legal documents) where summarization might involve different semantic operations.
4. **Limited Neuron-Level Intervention:** While we identified key neurons (particularly neuron 304) with significant activation changes, systematic ablation studies across combinations of neurons were not conducted. Our targeted LoRA interventions at the layer level (rather than individual neurons) serve as an indirect validation of the circuit hypothesis.

6 Ethical Considerations

We acknowledge several ethical dimensions of this research:

1. **Computational Resources:** This research utilized NVIDIA A100/A16 GPUs with an estimated carbon footprint of approximately 45kg CO₂eq for all experiments, reinforcing the value of parameter-efficient methods like targeted LoRA.
2. **Dataset Usage:** We used the publicly available CNN/DailyMail dataset in accordance with its terms of use for research purposes.
3. **Transparency:** Our code, trained models, and analysis pipeline will be made publicly available to ensure reproducibility and facilitate further research in mechanistic interpretability.
4. **Dual Use:** While our interpretability methods are designed to improve understanding of language models, similar techniques could potentially be used to identify vulnerabilities. We advocate for responsible use focused on improving model reliability and transparency.

Our research underscores the importance of interpretability for building more reliable and transparent language models, particularly for critical tasks like summarization where information selection has significant downstream impacts.

References

- Kevin Clark, Urvashi Khandelwal, Omer Levy, and Christopher D. Manning. 2019. What does BERT look at? an analysis of bert’s attention. In *Proceedings of the 2019 ACL*, pages 276–286.
- Kevin Clark, Minh-Thang Luong, Quoc V. Le, and Christopher D. Manning. 2020. Transformer interpretability beyond attention. In *NAACL*.
- Finale Doshi-Velez and Been Kim. 2017. Towards a rigorous science of interpretable machine learning. *arXiv preprint arXiv:1702.08608*.
- Alexander Elhage, Jan Leike, Miljan Martic, and 1 others. 2021. A mathematical framework for transformer circuits. *arXiv preprint arXiv:2106.13316*.
- Nelson Elhage, Tristan Hume, Catherine Olsson, Nicholas Joseph, Noor Siddiqui, Ben Goldhaber, Dario Amodei, Tom Brown, Jackson Kernion, Sam McCandlish, and Chris Olah. 2022. Toy models of superposition. *arXiv preprint arXiv:2209.10652*.
- Karl Moritz Hermann, Tomas Kocisky, Edward Grefenstette, Lasse Espeholt, Will Kay, Mustafa Suleyman, and Phil Blunsom. 2015. Teaching machines to read and comprehend. In *Advances in Neural Information Processing Systems*, volume 28, pages 1693–1701.
- Edward J. Hu, Yelong Shen, Phillip Wallis, Zeyuan Allen-Zhu, Yuanzhi Li, Shean Wang, and Wang Chen. 2021. Lora: Low-rank adaptation of large language models. *arXiv preprint arXiv:2106.09685*.
- Sarthak Jain and Byron C. Wallace. 2019. Attention is not explanation. In *Proceedings of the 2019 Conference of the North American Chapter of the Association for Computational Linguistics*, pages 3543–3556.
- Xiaoran Liu, Hang Yan, Shuo Zhang, Chenxin An, Xipeng Qiu, and Dahua Lin. 2024. Scaling laws of rope-based extrapolation. *arXiv preprint arXiv:2310.05209*.
- Yang Liu and Mirella Lapata. 2020. Fine-grained control of abstractive summarization via guided decoding. In *ACL*.
- Chris Olah, Shan Carter, Ludwig Schubert, and 1 others. 2020. The building blocks of interpretability. *Distill*.
- Alec Radford, Jeffrey Wu, Rewon Child, David Luan, Dario Amodei, and Ilya Sutskever. 2019. Language models are unsupervised multitask learners. Technical report, OpenAI.
- Aaditya K. Singh, Ted Moskovitz, Felix Hill, Stephanie C. Y. Chan, and Andrew M. Saxe. 2024. What needs to go right for an induction head? a mechanistic study of in-context learning circuits and their formation. *arXiv preprint arXiv:2404.07129*.
- Jianlin Su, Yu Lu, Shengfeng Pan, Bo Wen, and Yunfeng Liu. 2021. Roformer: Enhanced transformer with rotary position embedding. *arXiv preprint arXiv:2104.09864*.
- Hugo Touvron, Thibaut Lavril, Gautier Izacard, Xavier Martinet, Marie-Anne Lachaux, Timothée Lacroix, Baptiste Rozière, Naman Goyal, Eric Hambro, Faisal Azhar, Andrea Rodriguez, and 1 others. 2023a. Llama: Open and efficient foundation language models. *arXiv preprint arXiv:2302.13971*.
- Hugo Touvron, Louis Martin, Kevin Stone, Peter Albert, Amjad Almahairi, Yasmine Babaei, Nikolay Bashlykov, Soumya Batra, Prajjwal Bhargava, Shrutu Bhosale, Andrea Rodriguez, and 1 others. 2023b. Llama 2: Open foundation and fine-tuned chat models. *arXiv preprint arXiv:2307.09288*.
- Jakob Vig. 2019. A multiscale visualization of attention in the transformer model. In *Proceedings of the 57th Annual Meeting of the Association for Computational Linguistics*.
- Shuai Wang, Ming Zhong, and Wei Fan. 2021. Explainable abstractive summarization with transformer models. In *Proceedings of the AAAI Conference on Artificial Intelligence*.
- Bowen Yang, Bharat Venkitesh, Dwarak Talupuru, Hangyu Lin, David Cairuz, Phil Blunsom, and Acyr Locatelli. 2025. Rope to nope and back again:

A new hybrid attention strategy. *arXiv preprint arXiv:2501.18795*.

Wenxuan Zhao, Xuan Wang, Yun Liu, and 1 others. 2021. Contextualizing generative pre-trained transformers for document summarization. In *EMNLP*.